ARTICLES

A First Principles Analysis of the Location and Affinity of Protons in the Secondary Structure of Phosphotungstic Acid

Michael J. Janik, Robert J. Davis, and Matthew Neurock*

Department of Chemical Engineering, University of Virginia, Charlottesville, Virginia 22904-4741

Received: January 12, 2004; In Final Form: April 27, 2004

Nonlocal gradient corrected density functional theory was used to determine the optimal positions of the protons and their relative affinity in the secondary structure of phosphotungstic acid. First, a body centered cubic structure associated with the hexahydrate was incorporated into the model. The desorption energies of the first and second water molecules from a bridging $H_5O_2^+$ species were calculated to be 109 and 55 kJ mol^{-1}, respectively. The H_3O^+ or H^+ species remaining after dehydration are preferentially located between two oxygen atoms of adjacent Keggin units. The preferred position is between two terminal O_d atoms or between a terminal O_d atom and a bridging O_c atom, depending on the alignment of the Keggin units. The energy advantage of sharing a proton between two Keggin units is in the range of 43 to 71 kJ mol^{-1}. Three-dimensional periodic calculations indicate that anhydrous phosphotungstic acid can form a regular lattice in which all protons are shared between the heteropolyanions.

Introduction

Solid heteropolyacids (HPAs) offer an environmentally friendly solution to the corrosive liquids currently used in acid-catalyzed reactions, such as alkylations.[1−4] Rapid deactivation of these catalysts, however, has limited their industrial use.[5] As the acid strength can be linked to the position of the proton and the extent of hydration,[1] this deactivation may be in part due to structural changes of the bulk solid HPA and the arrangement of water molecules of hydration.

Heteropolyanions having the Keggin structure [Keggin unit (KU), chemical formula $XM_{12}O_{40}^{n-}$, Figure 1] are most often studied because of their stability, acid strength, and availability with respect to other forms of polyoxometalates. Phosphotungstic [$PW_{12}O_{40}^{3-}$ anion (PW), $H_3PW_{12}O_{40}$ (HPW) in the anhydrous acid form] is the strongest acid of the common Keggin units.[1,2,6] Many published reviews discuss the primary structure of this heteropolyanion.[2,4,7] There are four types of oxygen atoms in the KU: four in the central tetrahedron (O_a), twelve that bridge addenda atoms not sharing a central oxygen atom (corner-sharing, O_b), twelve that bridge two addenda atoms sharing the same central oxygen atom (edge-sharing, O_c), and twelve terminal oxygen atoms (O_d) associated with a single addendum atom. Figure 1 illustrates the positions of each type of oxygen atom. The bridging (O_b and O_c) and terminal (O_d) oxygen atoms are on the periphery of the structure and therefore are available to associate with protons or water molecules of hydration.

Assembly of the heteropolyanions with acidic protons, other cations, and/or water molecules into a regular solid forms the so-called secondary structure. A relatively stable form of hydrated HPW contains six water molecules per KU. The structure of this solid has been characterized by many methods, including single-crystal X-ray and neutron diffraction,[8] powder X-ray diffraction,[9,10] nuclear magnetic resonance (NMR) spectroscopy,[11−13] and Fourier transform infrared (FT-IR) spectroscopy.[14,15] The hexahydrate has a body-centered cubic (BCC) structure with KUs at the lattice points and $H_5O_2^+$ bridges along the faces. Each of the 12 terminal oxygen atoms of the KU is bound to a hydrogen atom of an $H_5O_2^+$ bridge. In this structure, the acidic protons are located in the $H_5O_2^+$ bridges.[8]

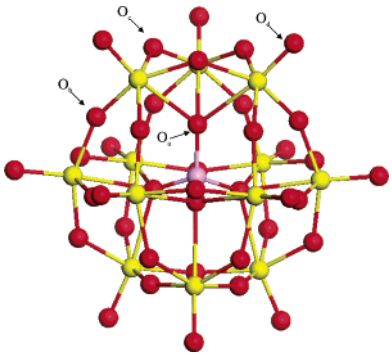

Figure 1. The Keggin structure of $PW_{12}O_{40}^{3-}$, identifying the four types of oxygen atoms in the structure.

Dehydration of the hexahydrate species begins just above room temperature and continues past 500 K.[6] If less than six water molecules per KU are present in the structure, acidic protons may be located in the remaining $H_5O_2^+$ bridges, in coordinated H_3O^+ species, or on the structural oxygen atoms of the KU.[1,16] In the anhydrous state, acidic protons are associated with structural oxygen atoms of the HPA. Thus, the acidic proton may participate in catalytic reactions from a hydrated state or an anhydrous oxide surface, depending on reaction conditions.

* Address correspondence to this author. E-mail: mn4n@virginia.edu.

10.1021/jp049843t CCC: $27.50
Published on Web 07/27/2004

A unique feature of solid HPA catalysts is their molecular nature. Computational and experimental studies have correlated the acidic properties to the elemental composition of the heteropolyanion.[2,6] However, the arrangement of these molecular units into a bulk structure also affects their catalytic behavior. The secondary structure and hydration state can change because of pretreatment or time on stream during reaction, which can affect the performance of the catalyst. For example, the rates of 1-butene isomerization (at 348 K) and pentane skeletal isomerization (at 473 K) over HPW decreased with time on stream and with increasing pretreatment temperature of the catalyst. Upon exposure of a deactivated catalyst to gas-phase water, up to 90% of the initial activity was regained.[17] FT-IR spectroscopy and microcalorimetry of water sorption showed that changes in hydration state were reversible with exposure to gas-phase water at 373 K after heating to 473 K, but were not reversible after heating to 573 K, despite the stability of the KU structure throughout this temperature range.[18] In addition, the proton conductivity of the HPW hexahydrate as a function of temperature was shown to reach a maximum at approximately 453 K.[19] Dehydration at higher temperatures was detrimental to proton conductivity. A detailed understanding of the location and nature of the protonic site in the HPA secondary structure is necessary for improving the performance of these materials.

Infrared spectroscopy,[20,21] ^{17}O NMR spectroscopy,[1,22] and density functional theory (DFT) quantum chemical calculations[6,23] have been used to explore the location of the protons on the KU. In a previous paper,[18] we used DFT calculations to determine the proton affinity of various oxygen atoms and show that the anhydrous proton can be located on bridging or terminal oxygen atoms. The energy difference between these sites is small and depends on the relative location of the other protons. In that study, we examined the interaction of protons with a single molecular KU, and did not consider the possibility of the acidic proton bridging between multiple KU in the bulk form.

Herein we report on DFT quantum chemical results for the bulk forms of anhydrous and hydrated phosphotungstic acid in which protons and water molecules bridge between KUs. The energies of desorption of water molecules from the hexahydrate form are computed, and the favorable geometries for the various stages of hydration are determined. The results are compared to X-ray diffraction (XRD) patterns and previously published water sorption microcalorimetry results.

Computational Methods

The minimum energy and optimized geometry for each structure were determined by using gradient corrected density functional theory as implemented in the Vienna ab initio Simulation Package (VASP) using plane wave basis sets.[24] Within the VASP formalism, ultrasoft pseudopotentials were used to describe electron−ion interactions,[25] and exchange and correlation energies were calculated by using the Perdew−Wang (PW91) form of GGA.[26] A $1 \times 1 \times 1$ Monkhorst−Pack mesh was used to sample the first Brillouin zone.[27] The energy change with larger *k*-point sampling was less than 0.01 eV with use of a $2 \times 2 \times 2$ mesh. A cutoff energy of 396.0 eV for the plane wave basis set was used in all calculations, which converges the total energy to less than 0.03 eV. Full geometry optimization was performed for each structure examined.

The supercell was constructed to represent the periodicity of the structure. The lattice vector optimization was performed manually. The lattice vectors examined were spaced by 0.1 Å, leaving an uncertainty of ±0.1 Å for the optimal value. For calculations in which one-dimensional periodicity was used, the supercell was tetragonal and the lattice vectors in the nonperiodic directions were 20 Å in length. This provides greater than 8 Å of vacuum space between closest atoms in neighboring cells along the nonperiodic directions. Three-dimensional calculations were run such that the supercell contained the desired periodicity in all directions. All calculations were performed with a single KU basis (with associated protons and water molecules) and all relative energies are reported on a per KU basis.

The energy of water desorption from the hexahydrate is defined as the difference in energy between the HPW·$(n-1)$-H_2O and H_2O species minus the energy of the HPW·nH_2O complex (eq 1).

$$\Delta E_{\mathrm{des}} = (E_{\mathrm{H_2O}} + \mathrm{E}_{\mathrm{HPW\cdot(}n-1\mathrm{)H_2O}} - \mathrm{E}_{\mathrm{HPW\cdot nH_2O}}) \qquad (1)$$

A positive value of ΔE_{des} indicates an endothermic desorption process whereas a negative value indicates an exothermic process.

Experimental Methods

Materials. Phosphotungstic acid hydrate, $H_3PW_{12}O_{40}\cdot xH_2O$, was obtained from Aldrich. Samples were dissolved in deionized and distilled water and then recrystallized by evaporating to dryness with moderate heating over a hot plate.

X-ray Diffraction. Powder X-ray diffraction studies were conducted on a Scintag XDS 2000 diffractometer, using a Cu Kα source with a wavelength of 0.154060 nm. The X-ray patterns were collected with a scan rate of 1 deg min^{-1} and a step size of 0.03°. To explore the effects of heating on the diffraction pattern, a sample was preheated in a convection oven for 3 h at 573 K with air flowing over the sample at 125 mL min^{-1}. The peak positions were corrected by using silicon powder (Aldrich) as an internal standard.

Thermal Gravimetric Analysis. Thermal gravimetric analysis (TGA) of the samples used for XRD experiments was used to determine the water content. Experiments were conducted on a TA Instruments 2050 Thermal Gravimetric Analyzer with helium (BOC Gases, grade 5, purified with Supelco OMI filter) flowing at 100 mL min^{-1}. The temperature program was a simple linear ramp from 303 to 873 K at a rate of 10 K min^{-1}. Approximately 400 mg of sample were used for each analysis.

Results and Discussion

Dehydration of the Bulk Hydrated State. The hydrated phase of HPW is a function of temperature and relative humidity.[28,29] However, higher hydrates will lose water to form the hexahydrate in the temperature range of 313−333 K.[10] Since solid acid catalyzed reactions are typically performed at temperatures near or above this range, consideration of the HPW solid structure will begin with the hexahydrate.

The positions of the atoms in the body centered cubic (BCC) structure of the hexahydrate of phosphotungstic acid ($H_3PW_{12}O_{40}\cdot 6H_2O$) were optimized, as illustrated in Figure 2. Figure 2A shows a face of the cubic structure and Figure 2B shows the relation to the body centered KU. This structure may be thought of as two interpenetrating cubic structures of anions sharing $H_5O_2^+$ cations, with no hydrogen bonding between the two. This is shown schematically in Figure 3. The $H_5O_2^+$ cations are shared between four KUs on the face of a cube. Hydration water molecules are not shared between the vertex KU and its nearest neighbor body centered KU. The H^+ of an $H_5O_2^+$ species associated with a body centered KU is located at the midpoint of an edge of the conventional unit cell. For these calculations,

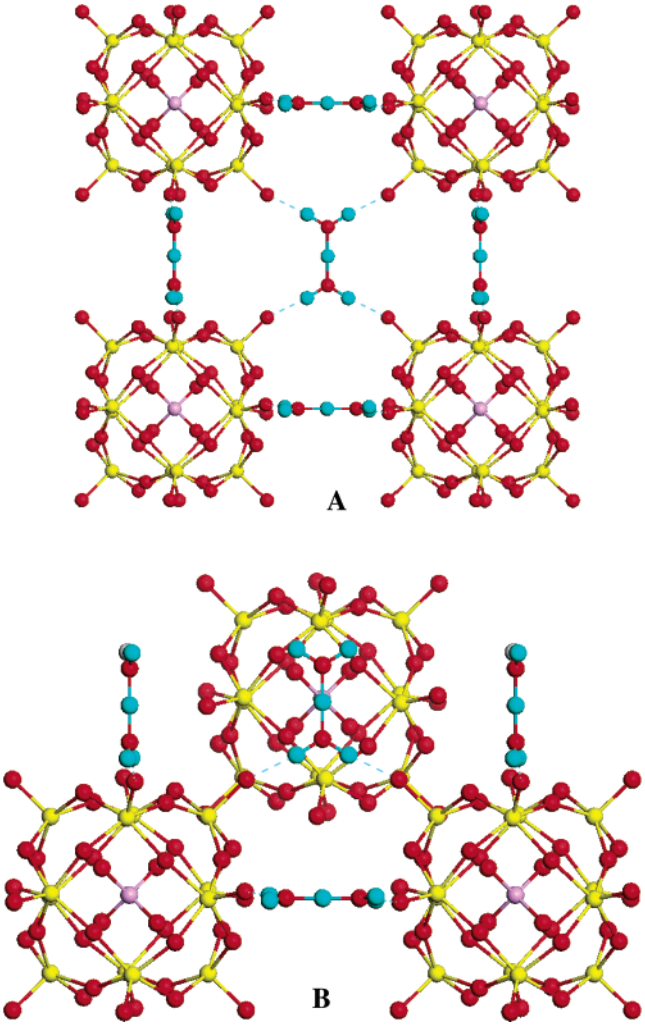

Figure 2. The optimized BCC structure of the hexahydrate $H_3PW_{12}O_{40}\cdot 6H_2O$. In this structure, all O_d atoms are bound to an $H_5O_2^+$ species; however, many of these species are left off the figure for simplification. (A) The view of one face of the BCC structure. (B) The relationship between KUs on an edge of the cube and the nearest neighbor body centered Keggin unit.

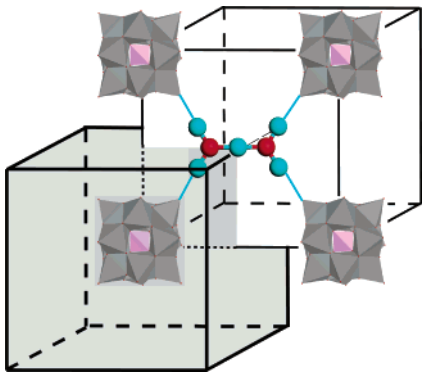

Figure 3. Schematic diagram illustrating the BCC structure of the hexahydrate $H_3PW_{12}O_{40}\cdot 6H_2O$ as two interpenetrating simple cubic structures. The H^+ of an $H_5O_2^+$ species coordinated to the body centered KU is located at the midpoint of an edge of the conventional cubic cell. The KUs are shown in polyhedral representation.

a BCC supercell with lattice constant *a* was used. The optimized value of *a*, 12.5 ± 0.1 Å, is similar to the experimentally determined lattice constant of 12.15 Å.[8] The optimized bond lengths for the KU within this structure are presented in Table 1. Table 2 presents the interatomic distances associated with the hydration water molecules, as labeled in Figure 4. The

TABLE 1: Comparison of Bond Lengths for the Keggin Unit of Phosphotungstic Acid

	bond length, Å		
bond	experiment[a]	VASP mol. − DFT[b]	VASP per. − DFT[c]
$W{=}O_d$	1.70	1.72 ± 0.001	1.73 ± 0.002
$W{-}O_c$	1.91	1.93 ± 0.002	1.92 ± 0.002
$W{-}O_b$	1.90	1.93 ± 0.003	1.92 ± 0.002
$W{-}O_a$	2.43	2.48 ± 0.010	2.48 ± 0.002
$P{-}O_a$	1.53	1.54 ± 0.001	1.54 ± 0.000

[a] Experimental values refer to those measured for the hydrated BCC structure $H_3PW_{12}O_{40}\cdot 6H_2O$.[8] [b] Lengths calculated with VASP for $PW_{12}O_{40}^{3-}$ isolated in a 20 × 20 × 20 Å^3 supercell.[18] Standard deviations are given because molecular symmetry was not enforced. [c] Lengths calculated with VASP for $H_3PW_{12}O_{40}\cdot 6H_2O$ in a BCC structure with optimized lattice constant $a = 12.5$ Å. Standard deviations are given because molecular symmetry was not enforced.

TABLE 2: Interatomic Distances Associated within the $H_5O_2^+$ Species of $H_3PW_{12}O_{40}\cdot 6H_2O$[a]

	exp[8]	VASP − DFT
$W{-}O_d$	1.70	1.74
$O_d{-}H_w$	1.72	1.82
$H_w{-}O_w$	0.95	0.99
$O_w{-}H^+$	1.19	1.20

[a] Atoms labeled as in Figure 4.

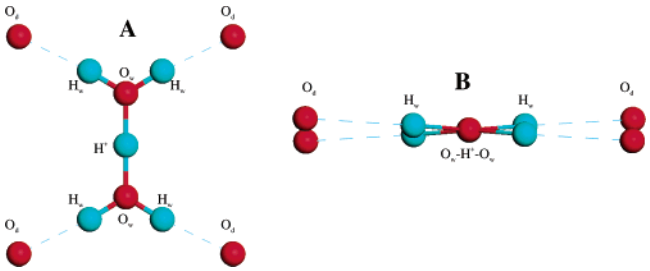

Figure 4. Results from the optimized $H_3PW_{12}O_{40}\cdot 6H_2O$ structure showing the geometry of the $H_5O_2^+$ species. (A) View in the plane of a face of the BCC structure. (B) View along the $O_w{-}H^+{-}O_w$ axis showing the out of plane twist. See Table 2 for the interatomic distances.

nearest neighbor phosphorus−phosphorus distance within this structure is approximately 10.8 Å.

It should be noted that the BCC arrangement in this study only approximates the known structure, since the body centered KU is actually inverted with respect to those on the vertexes of the cube. This slight modification to the structure minimally changes the configuration between structural oxygen atoms of nearest neighbor KUs. The shortest oxygen−oxygen distance of neighboring KUs was calculated to be 3.09 Å for an $O_c{-}O_d$ pair as opposed to 3.21 Å found experimentally.[8] A repulsive interaction may account for the larger calculated optimal lattice constant, which results in the slightly larger distances between O_d atoms and the water molecules of hydration. Since the $H_5O_2^+$ species do not bridge between nearest neighbors, this small difference does not affect the arrangement with the water molecules of hydration.

As mentioned earlier, solid HPA catalyzed reactions are often performed at temperatures that result in a hydration level between the hexahydrate and the anhydrous form. The initial loss of water converts an $H_5O_2^+$ species into an H_3O^+ species. Though the optimum position of $H_5O_2^+$ in the hexahydrate is well-characterized experimentally, little evidence exists for the position of the H_3O^+. On the basis of results from infrared spectroscopy, Paze et al. proposed that protons are tightly bound to the KU ($OH\cdots OH_2$) rather than forming weakly interacting hydronium ions (H_3O^+) at intermediate hydration states.[15]

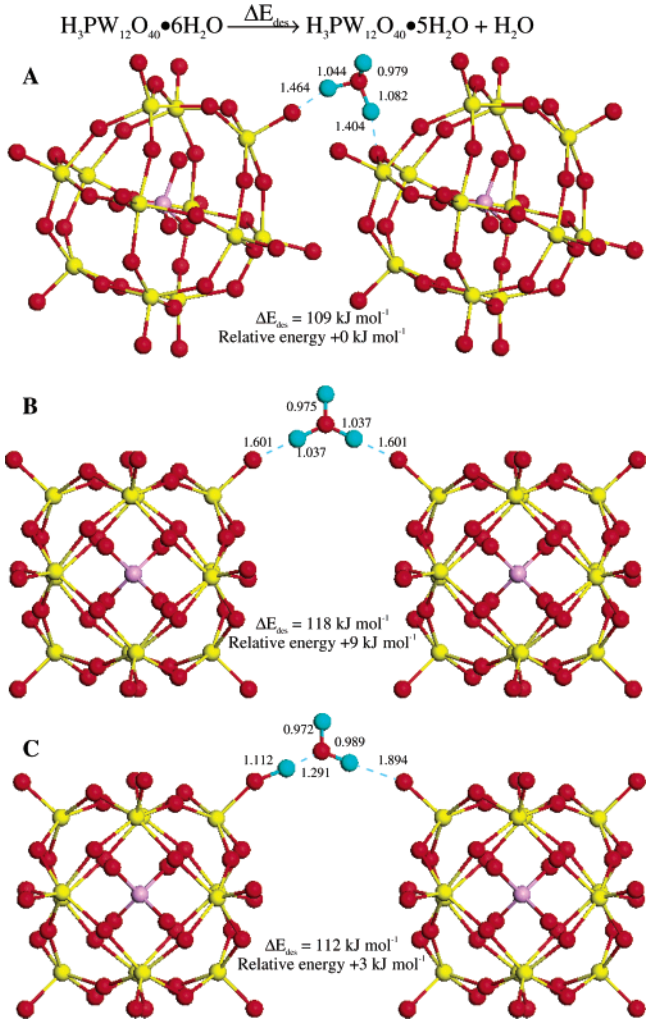

Figure 5. Structures resulting from the removal of one of the six water molecules of hydration from $H_3PW_{12}O_{40}\cdot 6H_2O$. The remaining H_3O^+ species location is (A) bridging between an O_d atom and an O_c atom of the nearest neighbor body centered KU, (B) bridging two O_d atoms of KUs across the edge of the cubic structure, and (C) bound to one of the two O_d atoms with a longer hydrogen bond to the second O_d atom. Relative energies are given with respect to the optimal configuration in part A. All distances are in angstroms. There are two remaining $H_5O_2^+$ species per KU that are not shown.

However, Misono inferred from ^{31}P NMR shifts that H_3O^+ is only weakly associated with the KU and suggested the possibility of H_3O^+ bridging between KUs.[4] Previous quantum chemical calculations indicate that, on a single KU, the optimum geometry is more representative of a water molecule coordinated to a bound proton than a loosely bound hydronium ion.[18]

The position and nature of the proton in intermediate hydration states can be studied by successive removal of water molecules from the hexahydrate structure. Thus, the energies of various structures with one of the six water molecules removed from the BCC structure were calculated. Figure 5 illustrates three configurations considered for the BCC structure with a water molecule removed. These correspond to H_3O^+ bridging between an O_d atom and an O_c atom of the nearest neighbor body centered KU (Figure 5A), H_3O^+ bridging equally between two O_d atoms of KUs across an edge of the cubic structure (Figure 5B), and H_3O^+ bridging unequally between the same two O_d atoms (Figure 5C). Although the three configurations are separated in energy by less than 10 kJ mol^{-1}, the first configuration is the lowest in energy. It represents H_3O^+ bridging between the closest two oxygen atoms in the structure. In the configuration of Figure 5B, the atoms of the remaining H_3O^+ species only slightly adjust their positions from those of the hexahydrate. It is energetically favorable for the species to adjust to nonsymmetric hydrogen bonding across the two O_d atoms (Figure 5C). It is then further favored for H_3O^+ to move to a position bridging nearest neighbor KUs (Figure 5A). The structure could not be optimized with an H_3O^+ species between two bridging oxygen atoms on adjacent KU because of the larger distance between these oxygen atoms and the proximity of terminal oxygen atoms. The energy of desorption of the first of the six water molecules of hydration is 109 kJ mol^{-1} for the most favorable structure (Figure 5A). This is approximately equal to the total value of adsorption of a second water molecule to form $H_5O_2^+$ on a single KU (-53 to -55 kJ mol^{-1} as calculated with VASP) plus two additional hydrogen bonds (-24 kJ mol^{-1} each, as calculated between two water molecules with VASP).

Various structures were optimized with a second water molecule of hydration removed, leaving an anhydrous proton. The proton cannot bridge between two O_d atoms across an edge of the cubic structure, as these two oxygen atoms are too far apart. Therefore, structures with the proton in the area between nearest neighbor KUs were considered. Figure 6 illustrates the configurations considered for the BCC structure with two water molecules removed. The optimal position of the anhydrous proton was found to be the same as that of the H_3O^+ species, bridging between an O_d atom and an O_c atom of the body centered KU (Figure 6A). This position is the same as that proposed for the fourth (anhydrous) proton in the hexahydrate of tungstosilicic acid, a compound isomorphous with HPW hexahydrate.[8] The energy of desorption of the second of the six water molecules of hydration is 55 kJ mol^{-1}. A structure with the proton bridging between an O_c atom and an O_d atom of the body centered KU is 10 kJ mol^{-1} higher in energy than the optimal configuration (Figure 6B). A structure with the proton bridging between an O_b atom and an oxygen atom of a water molecule of hydration bound to the body centered KU is 12 kJ mol^{-1} higher in energy than the optimal configuration (Figure 6C). In these structures, the distances between the anhydrous proton and the oxygen atoms it bridges form a long−short pair, with the longer of the distances (1.732−1.990 Å) indicative of a hydrogen bond. The structure with the anhydrous proton on a single O_d atom (not shown) is 43 kJ mol^{-1} higher in energy than the optimal configuration. A stable structure could not be located with the proton in the area between nearest neighbor KUs and bound to a single oxygen atom, indicating a strong preference for the proton to bridge between KUs. Therefore, it can be concluded that the anhydrous proton prefers to bridge between two oxygen atoms in the space between nearest neighbor KUs rather than be isolated on an oxygen atom of a single KU. The energetic preference of this proton sharing is better estimated in a simplified model described in a later section.

Calculated desorption energies can be compared with previously reported results from water sorption microcalorimetry.[18] The uptake of water on a sample pretreated at 473 K was slightly greater than 3 molecules per KU with the water sorption energy ranging from -87 to -20 kJ mol^{-1}. After pretreatment at 573 K, the uptake of water was less than 0.7 molecules per KU with a maximum sorption energy of -66 kJ mol^{-1}. The higher uptake and larger range of sorption energies for the lower pretreatment temperature suggests the reformation of the hydrated structure. This is in agreement with the higher energy of desorption calculated for the first of the six waters of hydration (109 kJ mol^{-1}), which involved hydration of the

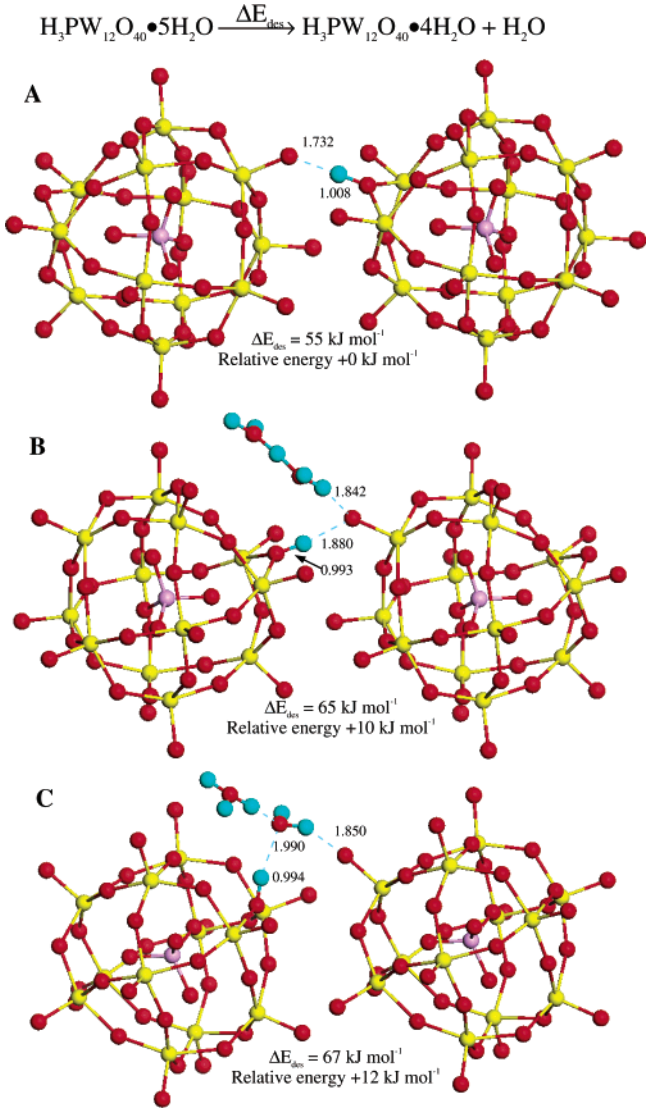

Figure 6. Structures resulting from the removal of two of the six water molecules of hydration from $H_3PW_{12}O_{40}\cdot 6H_2O$. The remaining anhydrous H^+ atom location is (A) bridging an O_d atom and an O_c atom of the nearest neighbor body centered KU, (B) bridging an O_c atom and an O_d atom of the nearest neighbor body centered KU, and (C) bridging an O_b atom and an oxygen atom of a water molecule of hydration bound to the nearest neighbor body centered KU. Relative energies are given with respect to the optimal configuration in part A. All distances are in angstroms. There are two remaining $H_5O_2^+$ species per KU and only those in close proximity to the anhydrous proton are shown.

proton along with the formation of the additional hydrogen bonds of the $H_5O_2^+$ species. The lower enthalpies were likely a result of hydrogen bonding between water molecules instead of directly hydrating a proton. The water sorption energy after pretreatment at 573 K is close to that calculated for desorption of a second water molecule. After pretreatment at the higher temperature, the water molecule might adsorb onto a proton bound to anhydrous HPW without formation of the additional hydrogen bonds of the BCC structure. Indeed, the low water uptake together with a low sorption energy suggest that the secondary hydrated BCC structure was not reconstituted in the experiment.

One-Dimensional Sharing of Protons between Keggin Units. Removal of water molecules creates the possibility that the BCC form of the secondary structure can change. Therefore, multiple crystal structures are considered for the anhydrous HPW. Before considering the three-dimensional anhydrous form, a one-dimensional array of KUs is examined. The one-dimensional system provides a simple model by which individual interactions can be examined. For example, the energy advantage for protons to bridge KUs and the repulsion associated with approaching KUs are each established with this one-dimensional model.

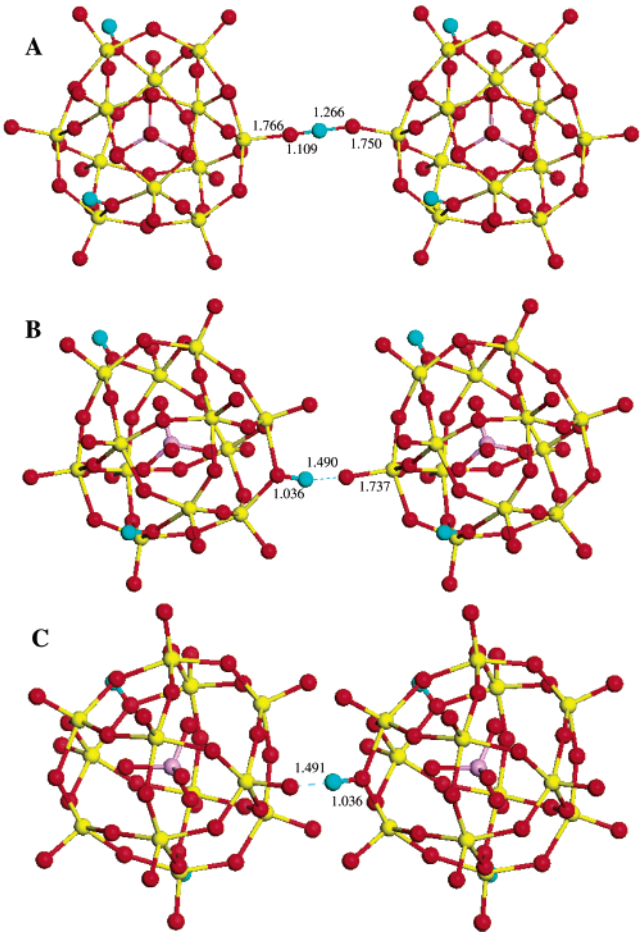

Figure 7. Optimized structures for proton sharing between two KUs in a one-dimensional lattice. (A) A proton is shared between two O_d atoms on adjacent KU. The P−P distance is 12.8 Å. (B) A proton is shared between an O_c atom and an O_d atom of an adjacent KU. The P−P distance is 11.5 Å. (C) A proton is shared between an O_c atom and an O_d atom aligned as nearest neighbors in the hexahydrate BCC structure. The P−P distance is 10.4 Å. All distances are in angstroms.

A cubic supercell of size $a \times 20 \times 20$ Å^3 is used, where a represents the lattice vector in the direction along which protons are shared. Two protons are located on oxygen atoms of a single KU, while the third is between two oxygen atoms of KUs in adjacent supercells. Figure 7 illustrates the configurations considered for one-dimensional bridging of protons between KUs. Sharing was considered in three different configurations, between two O_d atoms on adjacent KUs (Figure 7A) and in two configurations between an O_d atom and an O_c atom on adjacent KUs (Figure 7B,C). The first configuration (A) provides the simplest geometry for sharing of protons while maintaining the largest possible spacing between KUs (Figure 7a). The second configuration (B) provides the simplest one-dimensional sharing between an O_d atom and an O_c atom while maintaining a large KU spacing (Figure 7B). The third configuration (C) represents the alignment of nearest neighbor KUs in the hexahydrate BCC structure, with a proton shared between an O_d atom and an O_c atom (Figure 7C). The optimum lattice constant (i.e. the structure having the lowest total energy) was found to be 12.8 ± 0.1 Å for configuration A, 11.5 ± 0.1 Å for

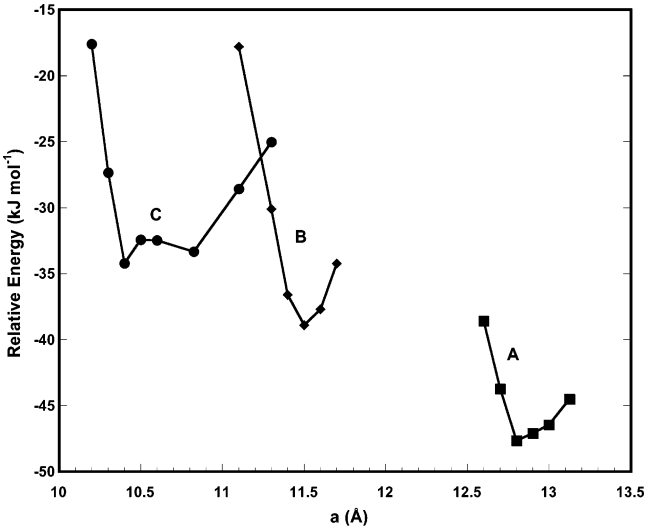

Figure 8. The relative energy of one-dimensional periodic structures with a proton bridging between two oxygen atoms on adjadent KU as a function of the lattice constant *a*. The energy is relative to the same structure with a lattice spacing of 20 Å, in which all protons are localized on a single KU. Negative values represent attractive interactions with respect to infinite spacing. Values are shown for the three configurations of Figure 7.

configuration B, and 10.4 ± 0.1 Å for configuration C. Figure 8 shows the relative energy of each configuration as a function of the lattice spacing *a*. The energy is relative to the same structure in a 20 × 20 × 20 Å^3 supercell, which does not allow for sharing between neighboring KUs. Negative values indicate that there is an attractive interaction to form the one-dimensional proton-sharing lattice.

The relative energy values in Figure 8 do not directly represent the true energy advantage of sharing protons between KUs, as these values are relative to an ideal, "infinitely" separated state. The repulsive interactions between the KUs must be considered as well. The repulsive energy is estimated by allowing KUs to approach each other in the one-dimensional lattice without proton sharing. The protons are moved to nonsharing locations and the lattice constant *a* is varied to determine the energy as a function of separation distance. This is done for each of the three configurations in Figure 7. The resulting repulsive interaction between KUs is plotted in Figure 9A as a function of the separation distance between KUs. In each case, as oxygen atoms on neighboring KUs are moved closer together, there is a repulsive interaction between the two KUs. The magnitude of the repulsion differs among configurations for a given value of *a*. However, it correlates well with the nearest oxygen−oxygen atom separation, irrespective of configuration (see Figure 9B). For configuration C, the interaction does not become repulsive until *a* is below 10.8 Å. The small "attractive" interactions at *a* greater than 10.8 Å are within the expected variation of the computational method.

The energy advantage of sharing protons between KUs versus locating protons directly on a single KU can be approximated as the difference in energy between the sharing and nonsharing configurations in the same lattice, relative to their respective energies in a 20 × 20 × 20 Å^3 supercell. The energy difference due to sharing of the proton can be approximated with eq 2

$$\Delta E_{\text{share}} = \text{RE}_{\text{sharing(1)}} - \text{RE}_{\text{nonsharing}} \qquad (2)$$

Here, RE refers to the relative energy values as shown in Figures 8 and 9. A negative value of ΔE_{share} represents a favorable sharing interaction. For sharing between two O_d atoms in

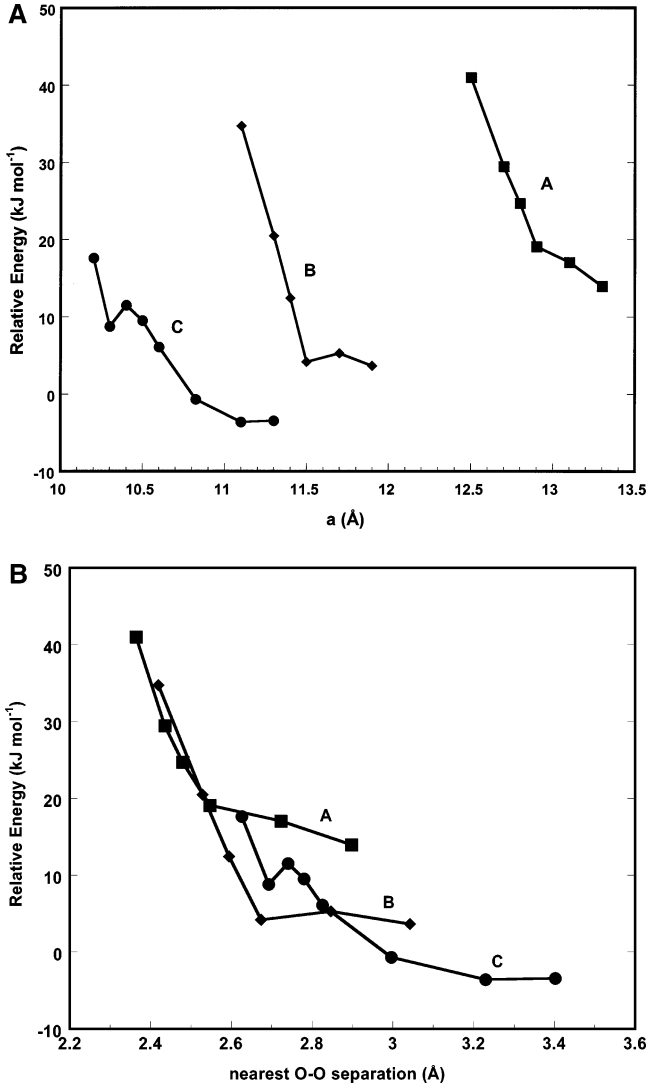

Figure 9. The relative energy of one-dimensional periodic structures in which KUs are separated by a lattice constant *a*. The energy is relative to the same structure with a lattice spacing of 20 Å. Positive values represent repulsive interactions with respect to infinite separation. Values are shown for the three configurations of Figure 7 with the proton bridging between KU moved to a nonbridging position. (A) relative energy versus the lattice constant *a*; (B) relative energy versus the nearest oxygen−oxygen atom distance of adjacent KUs.

configuration A, the sharing energy difference is $\Delta E_{\text{share}}^{O_d-O_d} = -71$ kJ mol $^{-1}$. For sharing between an O_d atom and an O_c atom the energy difference is −43 kJ mol^{-1} in configuration B and −46 kJ mol^{-1} in configuration C. The oxygen−oxygen distance is 2.4 Å for sharing between two O_d atoms in configuration A, and 2.5 Å for sharing between an O_d atom and an O_c atom in configurations B and C, with O−H−O angles of 179°, 169°, and 175°, respectively. These distances and angles are indicative of strong hydrogen bonds with little or no activation barrier for proton movement between the two oxygen atoms.[30,31]

The lack of an activation barrier is confirmed by using the nudged elastic band transition state search algorithm within VASP[32] for configuration A (Figure 7A). "Reactant" and "product" states were optimized with the proton nearer to each of the two O_d atoms involved, O_d−H- -O_d and O_d- -H−O_d. The energy difference between the two states is less than 0.5 kJ mol^{-1}. Four equally spaced images were optimized along the pathway of proton movement between the two sites with use of the nudged elastic band method. The energies of the four

images along the pathway differ by less than 0.5 kJ mol^{-1} from the "reactant" or "product" states and the force tangent to the reaction coordinate is less than 0.04 eV Å^{-1} for each image. Evidently, the proton is mobile between the two positions with a negligible activation barrier.

These results indicate that it is energetically favorable for anhydrous protons to bridge between adjacent KUs compared to a structure in which protons are bound directly to an oxygen atom of a single KU. A strong hydrogen bond that is formed between the KUs overcomes the repulsive interactions from bringing KUs near each other. In one dimension, this can occur in each of the three configurations (A, B, and C) presented in Figure 7. The three-dimensional anhydrous form is considered in the next section.

Though a one-dimensional array of KU is clearly a simplified system, these configurations may represent those available to supported KUs. The surface area of bulk HPW is small and many studies have explored the reactivity of HPW on various supports to increase the number of exposed acidic sites available for reaction.[33−35] X-ray diffraction results of 5 wt % of HPW on silica do not show a pattern indicative of bulk heteropolyacid crystallites, with the BCC structure pattern emerging at higher loading.[17] However, in the absence of a periodic structure, our one-dimensional lattice indicates that protons are likely to bridge between KUs in various configurations and with various spacings, as long as the oxygen atoms on two KUs can approach each other. This result can be qualitatively extended to KUs on a high surface area support as long as the loading level is such that KUs are in close proximity.

The Bulk Anhydrous State. The position of the anhydrous proton of HPW is still actively debated. With few exceptions, previous research has centered on the consideration of a localized proton on either a bridging or terminal oxygen atom of a single KU. On the basis of ^{17}O NMR results, Kozhevnikov concluded that the proton migrates between four equivalent terminal oxygen atoms linking KUs in a similar fashion as $H_5O_2^+$ in the hexahydrate.[22,36] Paze et al. inferred from infrared spectroscopy that the anhydrous proton may bridge between KUs in anhydrous HPW but that the spectra show no absorption compatible with the geometry proposed by Kozhevnikov.[15] Brown et al. proposed that the fourth (anhydrous) proton of tungstosilicic acid bridges between an O_c atom and an O_d atom in the hexahydrate structural analogue of HPW hexahydrate.[8] The infrared band of the O_d-H-O_c stretch in tungstosilicic acid has been assigned.[37] Here we consider the ability of the anhydrous proton to bridge between KUs in various three-dimensional crystal structures.

Simple cubic, tetragonal, and body centered cubic structures were explored for anhydrous HPW. In the simple cubic and tetragonal structures, protons are located in positions bridging between two O_d atoms on adjacent KUs, as illustrated in Figure 10. Though the KU positions in this structure appear similar to that of Figure 2A, substantial reorganization occurs between the body centered cubic and simple cubic forms. The orientation between nearest neighbor KUs is along the edge of the cube in the simple cubic crystal rather than along the body center diagonal. The simple cubic and tetragonal structures contain the geometry proposed by Kozhevnikov for four-way sharing of protons among terminal oxygen atoms.[36] In the anhydrous BCC structure, protons are located in positions bridging O_d and O_c atoms on nearest neighbor KUs, leaving the KUs in the same orientation as the hydrated BCC structure. The anhydrous BCC proton position is that proposed for sharing of a fourth proton in the BCC hexahydrate of tungstosilicic acid.[8]

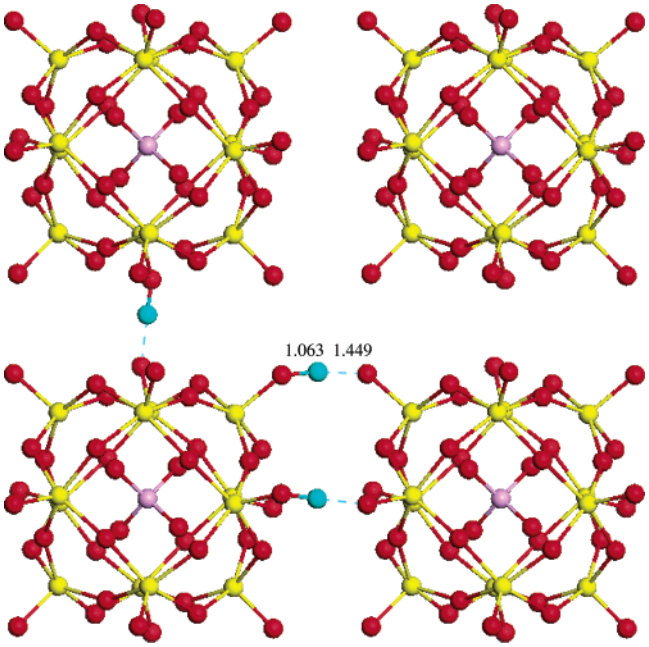

Figure 10. A plane of the optimized cubic structure of anhydrous $H_3PW_{12}O_{40}$. The P−P distance is 10.3 Å. Only protons of one KU (bottom left) are shown. All distances are in angstroms.

An optimized simple cubic structure is shown in Figure 10. The optimized lattice constant is 10.3 ± 0.1 Å, which represents a more compact structure than the hydrated state, since the P−P distance of neighboring KUs is decreased from 10.8 to 10.3 Å. This compact structure is necessary to bring the distance between the two O_d atoms to 2.5 Å. The energy advantage of placing an isolated anhydrous KU[18] into this three-dimensional crystal structure is −77 kJ mol^{-1}. There are four equivalent bridging positions between two O_d atoms in the plane shown in Figure 10. To address the mobility of the protons in this structure, an ab initio molecular dynamics calculation was performed. An ab initio molecular dynamics simulation was run starting from the optimized cubic structure at a beginning temperature of 298 K. A Nosé thermostat was used to control temperature fluctuations and a Verlet algorithm was used to integrate Newton's equations of motion. The simulation was run for 400 fs with a time step of 1 fs. During this time, the proton was found to be mobile, moving from a position between two terminal oxygen atoms to a position between one of these oxygen atoms and a third terminal oxygen atom in the plane of Figure 10. This simulation indicates the proton will likely move among the four equivalent positions. The simple cubic structure was also optimized whereby the proton is shared between the four O_d atoms in the center. However, this configuration was found to be substantially higher in energy.

In the tetragonal structure, the three protons are shared between KUs in two of the three cubic directions, leaving a third lattice vector unconstrained by hydrogen bonding. An optimal structure occurs with this third lattice vector extended to 11.0 ± 0.1 Å, which is 4 kJ mol^{-1} lower in energy than the simple cubic structure. It should be noted that the configuration of sharing between O_d atoms in the simple cubic and tetragonal three-dimensional structures differs from that presented above in one dimension. It is not possible to align KUs in a regular three-dimensional bulk structure so that protons are shared exactly as in Figure 7A, since O_d atoms do not approach each other in the other two directions.

The optimal lattice constant for the anhydrous BCC structure (12.5 ± 0.1 Å) was unchanged from that found for the hydrated

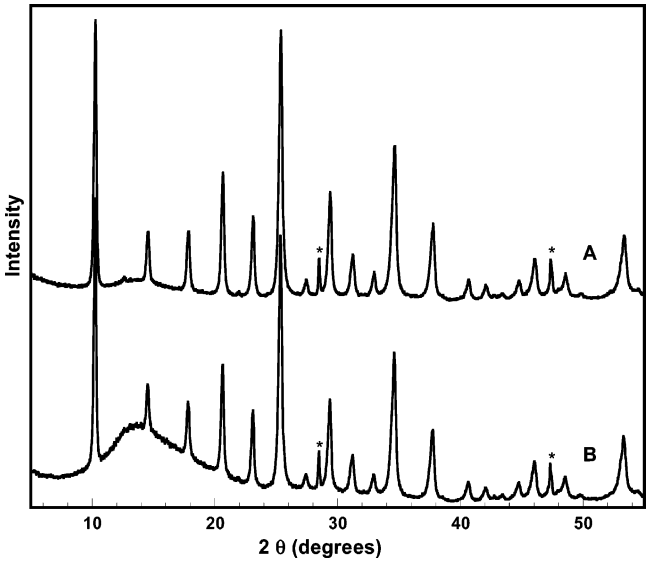

Figure 11. X-ray diffraction patterns for (A) HPW (recrystallized) and (B) HPW (recrystallized) pretreated for 3 h at 573 K. The asterisk (*) represents peaks due to Si powder used as a peak position reference.

structure. The energy advantage of placing an isolated anhydrous KU unto this three-dimensional structure is -99 kJ mol^{-1}, indicating this is the preferred anhydrous structure. The geometry in the vicinity of the shared protons is similar to that shown in Figure 6A. The nearest neighbor distance is 10.8 Å, which is larger than the optimal distance for sharing protons in this configuration in one dimension (Figure 7C). However, there are three proton sharing interactions and five nonsharing interactions for each KU in the BCC structure. By using the relative energies calculated in the one-dimensional case for a KU separation of 10.8 Å (from Figures 8 and 9A), each sharing interaction is valued at -33 kJ mol^{-1}, while each nonsharing interaction has a relative energy of -1 kJ mol^{-1}. Thus, an energy advantage relative to an isolated anhydrous KU of -103 kJ mol^{-1} is predicted for an anhydrous BCC structure with a lattice constant of 12.5 Å, which is close to the calculated relative value of -99 kJ mol^{-1}. Similarly, for an anhydrous BCC structure with a lattice constant of 12.1 Å, the three-dimensional calculated relative energy (-59 kJ mol^{-1}) and the relative energy predicted from one-dimensional sharing and nonsharing interactions (with a KU separation of 10.5 Å, -54 kJ mol^{-1}) agree. The one-dimensional interaction energies for a given configuration provide a reliable estimation of the interactions within a three-dimensional structure.

The computational results presented indicate that the phosphotungstic acid catalyst is likely to contain protons bridging between KUs. As these protons are located in the area between KUs, they will be more difficult for reactant molecules to access. Furthermore, as these positions are substantially favored over positions isolated on a single KU, the activation barrier to leaving these positions may be substantial. The deactivation of the HPW catalyst with dehydration may be due to the movement of protons to these inaccessible positions in the anhydrous state. A future study will address the mobility of the proton in HPW and the effect of water on the activation barrier for movement.

X-ray Diffraction Results. Figure 11 illustrates the X-ray diffraction patterns for recrystallized phosphotungstic acid (Figure 11A) and for a sample pretreated at 573 K for 3 h (Figure 11B). Thermal gravimetric analysis confirmed that the recrystallized sample contained 6 waters of hydration per KU. Furthermore, the TGA results indicated that the pretreated sample had approximately 3 waters of hydration per KU. Since all hydration water molecules are lost at 573 K, the pretreated sample partially rehydrated upon exposure to ambient conditions. Both samples exhibited the BCC crystal pattern of phosphotungstic acid.[8,16] The lattice constant was calculated to be 12.17 Å for both samples. The major difference in the pattern following pretreatment is the growth of a broad feature ranging over 2θ values from 8° to 24°. This feature suggests some loss of crystallinity following pretreatment. However, the peak positions and intensities of the BCC XRD pattern were not significantly altered, indicating the BCC structure is retained at the intermediate hydration level. These experiments agree with our computational results, which suggest that H_3O^+ species and anhydrous protons prefer to bridge between oxygen atoms on nearest neighbor KUs within the BCC structure, and therefore maintain the BCC structure following dehydration. Fournier et al. performed a series of in situ XRD studies on heteropolyacids, including HPW.[10] For HPW, a tetragonal phase appeared along with the cubic phase at 373 K. At 623 K only the tetragonal phase was present. The calculations presented above also show an anhydrous tetragonal phase to be energetically advantageous by allowing the sharing of protons between KUs. Fournier et al. also noted a return to the cubic phase for a sample that had been heated then treated with water at atmospheric conditions. However, the return of the BCC structure after heat treatments in our XRD experiments and those of Fournier et al. cannot be directly compared to results from FTIR spectroscopy and water sorption microcalorimetry performed previously.[18] Rehydration in those experiments was performed at 373 K rather than room temperature.

Conclusions

First principles density functional theory calculations were used to elucidate the crystal form and acidic proton position associated with the secondary structure of phosphotungstic acid as a function of hydration state. Results indicate that dehydration of the hexahydrate leads to H_3O^+ and H^+ species that preferentially bridge between nearest neighbor Keggin units in the BCC structure. The desorption of the first water molecule from the hexahydrate was found to be substantially more endothermic than desorption of a second water molecule. X-ray diffraction confirmed that the BCC structure was retained with three water molecules of hydration per Keggin unit. Computational results indicate that protons in the anhydrous structure also prefer to bridge between Keggin units. Calculations of interaction energies between Keggin units arranged in one dimension were found to accurately predict the energetics of forming a three-dimensional crystal structure.

Acknowledgment. This work was funded by the National Science Foundation (CTS-0124333).

References and Notes

(1) Kozhevnikov, I. V. *Russ. Chem. Rev.* **1987**, *56*, 811.
(2) Okuhara, T.; Mizuno, N.; Misono, M. *Adv. Catal.* **1996**, *41*, 113.
(3) Misono, M. *C. R. Acad. Sci., Ser. IIc, Chim.* **2000**, *3*, 471.
(4) Misono, M. *Chem. Commun.* **2001**, 1141.
(5) Misono, M.; Nojiri, N. *Appl. Catal.* **1990**, *64*, 1.
(6) Bardin, B. B.; Bordawekar, S. V.; Neurock, M.; Davis, R. J. *J. Phys. Chem. B* **1998**, *102*, 10817.
(7) Pope, M. T. *Heteropoly and Isopoly Oxometalates*; Springer-Verlag: New York, 1983.
(8) Brown, G. M.; Noe-Spirlet, M. R.; Busing, W. R.; Levy, H. A. *Acta Crystallogr.* **1977**, *B33*, 1038.
(9) Kremenovic, A.; Spasojevic-de Bire, A.; Dimitrijevic, R.; Sciabu, P.; Mioc, U. B.; Colomban, P. *Solid State Ionics* **2000**, *132*, 39.
(10) Fournier, M.; Feumi-Jantou, C.; Rabia, C.; Herve, G.; Launay, S. *J. Mater. Chem.* **1992**, *2*, 971.

(11) Maksimovskaya, R. I. *Kinet. Catal.* **1995**, *36*, 836.
(12) Uchida, S.; Inumaru, K.; Misono, M. *J. Phys. Chem. B* **2000**, *104*, 8108.
(13) Essayem, N.; Tong, Y. Y.; Jobic, H.; Vedrine, J. C. *Appl. Catal. A* **2000**, *194*−*195*, 109.
(14) Koyano, G.; Saito, T.; Hashimoto, M.; Misono, M. *Stud. Surf. Sci. Catal.* **2000**, *130*, 3077.
(15) Paze, C.; Bordiga, S.; Zecchina, A. *Langmuir* **2000**, *16*, 8139.
(16) Mioc, U.; Davidovic, M.; Tjapkin, N.; Colomban, P.; Novak, A. *Solid State Ionics* **1991**, *46*, 103.
(17) Bardin, B. B.; Davis, R. J. *Appl. Catal. A* **2000**, *200*, 219.
(18) Janik, M. J.; Campbell, K. A.; Bardin, B. B.; Davis, R. J.; Neurock, M. *Appl. Catal. A* **2003**, *256*, 51.
(19) Slade, R. C. T.; Omana, M. J. *Solid State Ionics* **1992**, *58*, 195.
(20) Lee, K. Y.; Mizuno, N.; Okuhara, T.; Misono, M. *Bull. Chem. Soc. Jpn.* **1989**, *62*, 1731.
(21) Essayem, N.; Holmqvist, A.; Gayraud, P. Y.; Vedrine, J. C.; Taarit, Y. B. *J. Catal.* **2001**, *197*, 273.
(22) Kozhevnikov, I. V.; Sinnema, A.; Van Bekkum, H. *Catal. Lett.* **1995**, *34*, 213.
(23) Ganapathy, S.; Fournier, M.; Paul, J. F.; Delevoye, L.; Guelton, M.; Amoureux, J. P. *J. Am. Chem. Soc.* **2002**, *124*, 7821.
(24) Kresse, G.; Furthmuller, J. *Phys. Rev. B* **1996**, *54*, 11169.
(25) Vanderbilt, D. *Phys. Rev. B* **1990**, *41*, 7892.
(26) Perdew, J. P.; Chevary, J. A.; Vosko, S. H.; Jackson, K. A.; Pederson, M. R.; Singh, D. J.; Fiolhais, C. *Phys. Rev. B* **1992**, *46*, 6671.
(27) Monkhorst, H. J.; Pack, J. D. *Phys. Rev. B* **1976**, *13*, 5188.
(28) Nakamura, O.; Ogino, I.; Kodama, T. *Mater. Res. Bull.* **1980**, *15*, 1049.
(29) Nakamura, O.; Ogino, I.; Kodama, T. *Solid State Ionics* **1981**, *3*−*4*, 347.
(30) Scheiner, S. *Acc. Chem. Res.* **1985**, *18*, 174.
(31) Kreuer, K. D. *Chem. Mater.* **1996**, *8*, 610.
(32) Mills, G.; Jonsson, H.; Schenter, G. K. *Surf. Sci.* **1995**, *324*, 305.
(33) Soled, S.; Miseo, S.; McVicker, G.; Gates, W. E.; Gutierrez, A.; Paes, J. *Chem. Eng. J.* **1996**, *64*, 247−254.
(34) De Angelis, A.; Amarilli, S.; Berti, D.; Montanari, L.; Perego, C. *J. Mol. Catal. A* **1999**, *146*, 37.
(35) Blasco, T.; Corma, A.; Martinez, A.; Martinez-Escolano, P. *J. Catal.* **1998**, *177*, 306.
(36) Kozhevnikov, I. V. *Catal. Lett.* **1994**, *27*, 187.
(37) Bielanski, A.; Datka, J.; Gil, B.; Malecka-Lubanska, A.; Micek-Ilnicka, A. *Catal. Lett.* **1999**, *57*, 61.